

1995

NASA/ASEE SUMMER FACULTY FELLOWSHIP PROGRAM

MARSHALL SPACE FLIGHT CENTER
THE UNIVERSITY OF ALABAMA IN HUNTSVILLE

MATHEMATICAL MODELING OF THE GAS AND POWDER FLOW IN THE
(HVOF) SYSTEMS TO OPTIMIZE THEIR COATINGS QUALITY

Prepared By: Hazem H. Tawfik, Ph.D., P.E., CMfg.E.
Academic Rank Professor and Director
Institution and Department State University of New York at Farmingdale
Manufacturing and Mechanical Research

NASA/MSFC:

Laboratory: Materials & Processes Laboratory
Division: Metallic Materials Division
Branch: Metals Processes Branch

MSFC Colleague: Frank Zimmerman

1. INTRODUCTION

Thermally sprayed coatings have been extensively used to enhance materials properties and provide surface protection against their working environments in a number of industrial applications. Thermal barrier coatings (TBC) are used to reduce the thermal conductivity of aerospace turbine blades and improve the turbine overall thermal efficiency. TBC allows higher gas operating temperatures and lower blade material temperatures due to the thermal insulation provided by these ceramic coatings. In the automotive industry, coatings are currently applied to a number of moving parts that are subjected to friction and wear inside the engine such as pistons, cylinder liners, valves and crankshafts to enhance their wear resistance and prolong their useful operation and lifetime.

Recently, hexavalent chromium associated with hard chromium plating, was classified as a human carcinogen and environmental pollutant. Aerospace industry has traditionally used hard chrome plating as a corrosion protection material. Accordingly, NASA is developing thermal spray coatings to replace the hard chrome plating that is currently being utilized on the space shuttle main engine. These coatings are made of tungsten carbide and cobalt, chromium oxide, and FerroTic (iron based material with titanium carbide) to provide protection against wear, corrosion and hydrogen embrittlement of the low pressure liquid hydrogen carrying ducts on the shuttle main engine. One of these sections is the Low Pressure Fuel Turbo Pump (LPFTP) discharge duct used on the shuttle main engine. The duct carries liquid hydrogen fuel at temperature of -253°C (-423°F) to the

High Pressure Fuel Turbopump from the (LPFTP) [1].

In addition to the extensive use of thermal spray in generating protective coatings, it has been used in the manufacturing of near-net shape parts with customized material and engineered properties. In these applications, thermal spray is used to build up material(s) to form the required part geometry. Moreover, thermal spray is used for the repair of worn or mis-machined mechanical parts.

Despite the considerable advancement in the thermal spray technology, the industry still faces strong challenges with the coatings quality in the following areas: 1) Delamination or debonding at the substrate/coating interface and intersplat boundaries - this usually occurs due to mechanical and thermal residual stresses caused by a mismatch in the thermal expansion coefficient combined with localized sharp temperature gradient due to a high cooling rate. 2) The occurrence of voids and porosity within the coatings - is usually caused by trapped gases and/or powder oxidation during spraying process. This will drastically weaken both the corrosion protection ability and the hardness of the thermally sprayed coatings. The porosity will allow the corrosive solution to penetrate the coating to the interface between the base material and the coating.

Thermally sprayed coatings are formed from the flattened consolidation and solidification of molten powder particles; thus, the properties of these coatings are highly

velocity of molten particles [2]. Critical review of the literature on thermal spray coatings, indicated that high velocity thermal spray processing conditions offer the best potential to minimize the occurrence of manufacturing related flaws and provide high quality coatings [3].

In recent years the High Velocity Oxygen Fuel (HVOF) system has been considered an asset to the family of thermal spraying processes Fig. (1). Especially, for spray materials with melting points below 3000 °K it has proven successful, since it shows economic advantages when compared to other coating processes that produce similar quality coatings [4]. In such systems that produce high velocity particles, the oxide content of the coatings did not correlate to the particle temperature or the excess oxygen in the lean fuel conditions, but it is related to high substrate temperatures [5]. It is believed that the primary mechanism for the formation oxide inclusions occurs after a particle splat, when the hot coating is exposed to the oxygen contained in the relatively low velocity boundary layer. The exposure times of a given splat to the boundary layer are on the order of seconds, a factor of 10^3 longer than during particle flight [6]. The usual evaluation of optimized spraying parameters, which include stand off distance, fuel and oxygen flow rates, powder size, and barrel length, are based on numerous, extensive, and expensive experiments laid out by trial-and-error or statistical design of experiments and Taguchi methods [4].

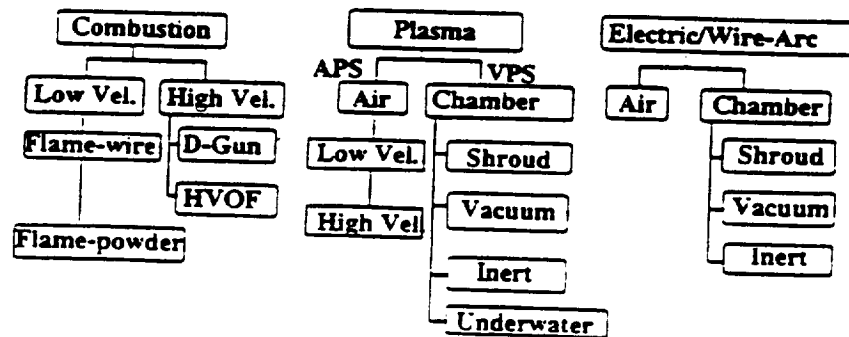


Figure 1. Thermal Spray processes

The application of simulation techniques to thermal spray processes has grown steadily over the past years because of the relatively inexpensive parametric analysis and operations. Once a model of the process is established and validated, system parameters become evident. The obtained fundamental understanding of the optimization process can be accomplished with a numerical computer model [4].

The objective of this investigation was to develop a computer model that simulates the thermal and gas dynamics of both gases and particles associated with the HVOF process to provide predictions of the particles velocities and temperatures. In the HVOF process oxygen and atomized kerosene are injected coaxially into the combustion chamber, Fig. (2), where they are mixed and ignited by a spark plug. The hot combustion gases are accelerated to supersonic conditions in a conversion diversion nozzle. At the exit of the nozzle the

powder is transversely injected with an argon or nitrogen carrier gas. The powder is heated and accelerated in the gun barrel and jet region by the hot gas and eventually is deposited on the substrate. The model was partially validated against the very limited experimental data collected from Hobart Tafa using the JP-5000 gun and shown in Figure (2).

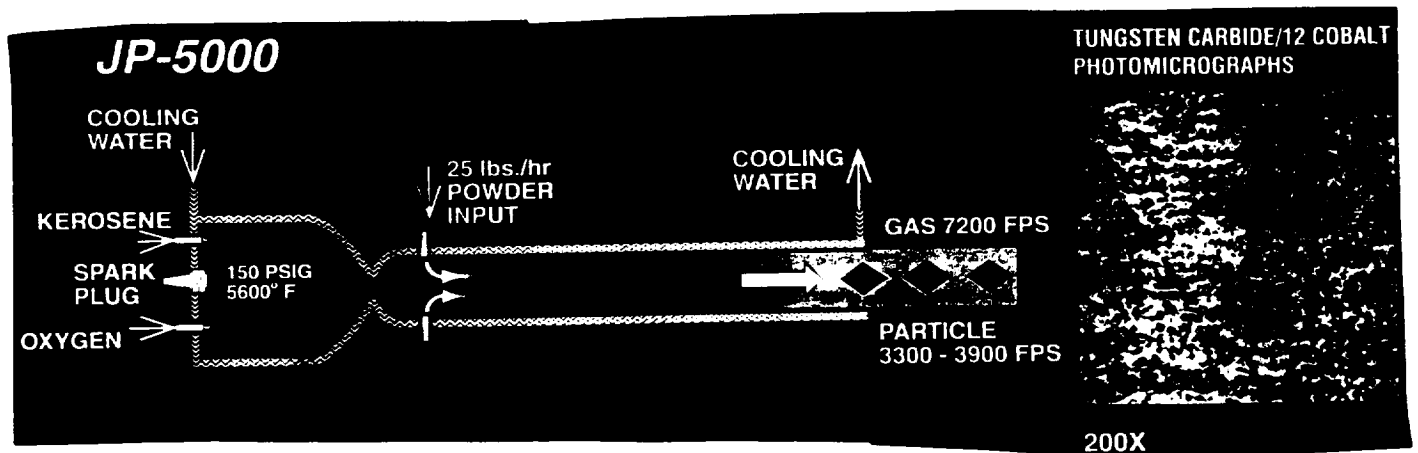


Fig.(2) Hobart Tafa HVOF/JP-5000 - with shown Numerical Values for Gas and Particle Velocity and Temperature

2. MATHEMATICAL MODEL

The current model development was accomplished in four main stages as described in the following :

First Stage: Modelling of the gases flow inside the HVOF system without initial consideration to the powder flow [7]:

The generalized flow equations with the influence parameters were used to model the gas flow in the HVOF system shown in Figure (2). The temperature and Mach Number equations (1), (2) were numerically integrated for a single phase non-adiabatic friction flow with variable specific heats [7].

$$\frac{dM^2}{M^2} = -2 \frac{(1 + \frac{k-1}{2} M^2)}{1-M^2} \frac{dA}{A} + \frac{1+kM^2}{1-M^2} \frac{dQ}{c_p T} + \frac{kM^2(1 + \frac{k-1}{2} M^2)}{1-M^2} 4f \frac{dx}{D} - \frac{dk}{k} \quad (1)$$

$$dT = (k-1) M^2 \frac{dA}{A} - (1-kM^2) \frac{dQ}{c_p T} - \frac{2(k-1)M^4}{1-M^2} \frac{dx}{D} \quad (2)$$

$$T = (1-M^2) \frac{A}{c_p T} - \frac{2(1-M^2)}{D} \frac{dx}{D}$$

Equations (1) and (2) above were solved by a numerical computer model and predictions of the gas velocity and temperature were obtained [7] at all the flow cross sections inside the

thermal spray system for the inlet conditions given in Fig. (1). Due to the appearance of the term $(1-M^2)$ in the denominator of equations (1) and (2), the numerical model experienced some degree of singularity in the vicinity of the throat section. The model quickly recovered as the solution propagated downstream of the throat area. However, this singularity problem could be completely rectified by the application of a Taylor series expansion on these terms in the throat proximity zone.

Second Stage: Empirical Correlation for the mean axial velocity and temperature decay of a free supersonic jet plume:

Visual studies such as Schlieren flow visualization showed a "potential core" with an embedded shock-diamond structure that is formed in the supersonic zone due to the underexpanded nature of the jet, Fig (3), [6]. Further down stream large turbulent eddies were generated by the large velocity and temperature gradients at the boundary layer between the jet and the ambient air. This mixing zone is further subjected to the effect of a large density difference between the hot jet core and the comparatively cold and slow ambient atmosphere. Small particles $5\ \mu\text{m}$ or smaller will fully track the turbulent motion of the fluid, however, much larger particles, such as typical HVOF metal spray powders, are generally unaffected by the eddies and remain in the relatively high temperature, low density, and least motion resistance zone near the jet centerline.

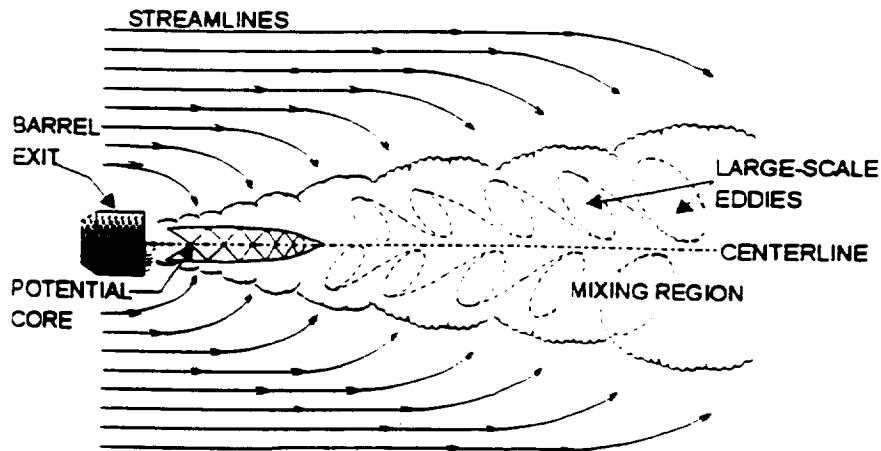


Fig. (3) Supersonic Jet Structure

In an attempt to better understand the noise generation mechanism in supersonic free jets, considerable investigation efforts have been devoted to the measurements of various flow parameters and the study of how these quantities vary with jet flow conditions [8]. Earlier mean velocity measurements [8] using laser velocimeter and hot-wire anemometer resulted in an empirical formula which gives the variation of the potential core length, Figure (3) with the Mach number for both heated and cooled jets, it read as follows:

$$\frac{x_c}{D} = 4.2 + 1.1 M_j^2 \text{ ----- (3)}$$

Another general empirical correlation for the supersonic axial mean velocity decay with range of validity between Mach Number 0.3 - 1.4., this correlation read as follows [8]:

$$\frac{U}{U_j} = 1 - \exp \left[\frac{1.35}{\left(1 - \frac{x}{x_c}\right)} \right] \text{ ----- (4)}$$

In the HVOF applications the jet mean axial velocity and temperature ranges are between (1.5 - 2.5 M) and (1500 - 3000° K) respectively. The recent study of the heated jets indicated that the potential core length decreased as the jet temperature increased [9]. Thus, correlations (3), and (4) were modified to expand their range of validity by correlating recent measurements of the mean axial decay velocity and temperature obtained from NASA/Langley [9] and University of Toronto [10]. Figures 4 and 4A show the mean velocity and temperatures correlations in relation to the measured values respectively. The comparison of these Figures 4, and 4A for free axisymmetrical jets indicated that the velocity decays faster than the temperature.

Third Stage: Momentum Transfer Mechanism Between Gas and Particle

The momentum equation, for either solid or liquid particles, are solved in a Lagrangian frame of reference moving with the particles. The equation of motion for the particle is written as [11]:

$$m_p \frac{dV_p}{dt} = \frac{1}{2} \rho_g A_p C_D (V_g - V_p) |V_g - V_p| - V_p \nabla p \text{ ----- (5)}$$

Where m_p is the mass of the particle and V_p is the velocity vector of the particle, C_D is the drag coefficient, and the particle motion in two-phase flows depends upon the gas properties, particle properties, and ρ_g , V_g , P are the density, velocity and pressure of the gas, respectively. A_p is the particle surface area and V_p is the particle volume. All particles are assumed to be spherical. This equation of motion for a particle accounts for the acceleration/deceleration of the droplet, due to the combined effects of drag from the gas flow, and local pressure gradients in the gas. Because the gas flow pressure change is small in the friction flow inside the gun barrel and the free jet plume, the gas pressure gradient effect on the particle motion is neglected in comparison to the drag force. A literature survey in the area of two-phase flows reveals that a number of drag coefficient equations have been used to calculate particle motion in supersonic flows [12]. Because the particles are initially injected into a supersonic flow, each particle will have a shock wave on the upstream side. The drag induced on these particles in this supersonic flow is calculated with the following

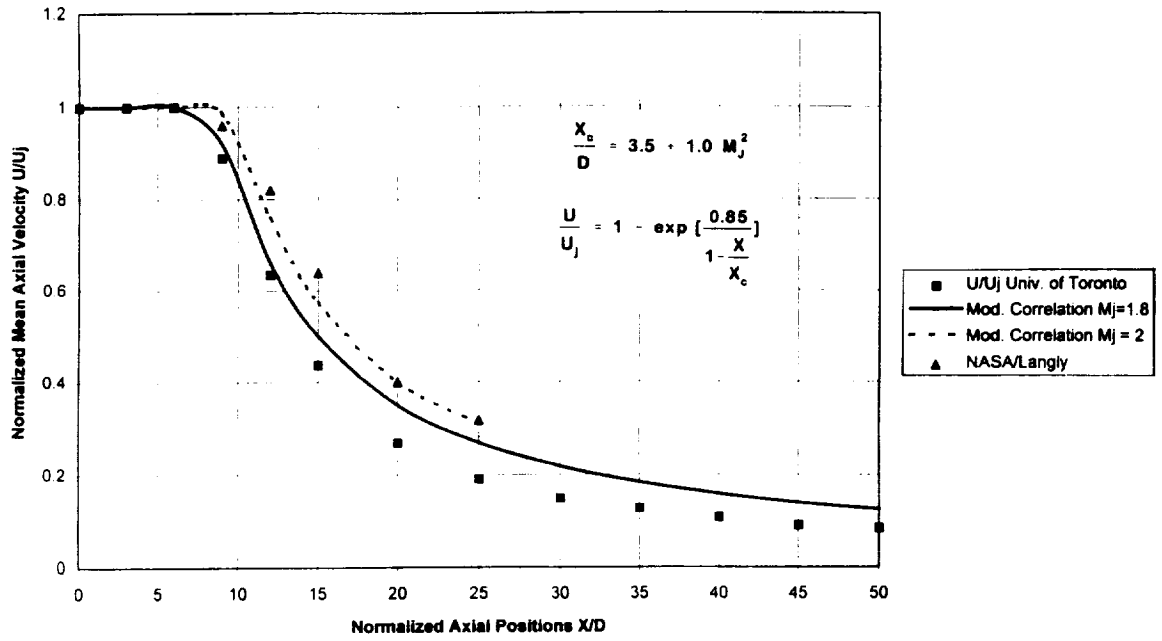


Figure (4) Modified Axial Decay Velocity in Supersonic Jet Plumes

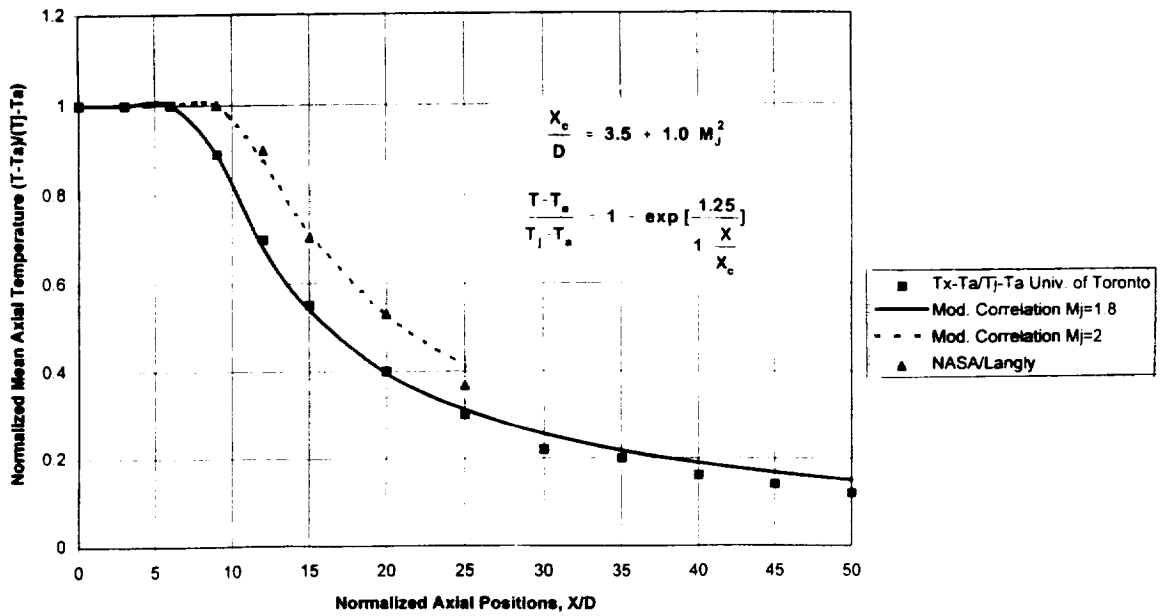


Figure (4A) Modified Axial Decay Temperature For Supersonic Jet Plumes

empirical correlation:

$$\frac{dV_p}{dt} = \frac{3}{4} C_D \left(\frac{\rho_g}{\rho_p} \right) \frac{(V_g - V_p) |V_g - V_p|}{d} \text{----- (6)}$$

The drag coefficient for the particle is based on the local Reynolds number of the particle and is evaluated as:

$$R_e = \frac{\rho |V_g - V_p| d_p}{\mu}$$

here μ is the molecular viscosity of the gas. The variation of the gas viscosity was evaluated from the graph and empirical formula shown in Figure (5). The following correlations have been found to be valid for a wide range of Reynolds number [11]; it reads as follows:

$$C_D = \frac{24}{R_e} \quad \text{for } R_e < 1$$

$$C_D = \frac{24}{R_e} (1 + 0.15 R_e^{0.687}) \quad \text{for } 1 < R_e < 10^3$$

$$C_D = 0.44 \quad \text{for } R_e > 10^3$$

Fourth Stage: Heat Transfer Mechanism Between The Gas and The Powder:

The coefficient of heat transfer (h) between the particle and the gas can be determined from the following Ranz-Marshall semiempirical equation:

$$Nu = \frac{hd_p}{k_g} = 2 + 0.6 Re^{.5} Pr^{0.3333} , \quad Pr = \frac{c_p \mu_g}{k_g}$$

Where c_p is the specific heat of combustion gases given by correlations shown in table (1), d_p is particle diameter, and k_g is the coefficient of gases thermal conductivity - it was evaluated from a correlation as a function of the temperature as shown in Figure (6). Considering that the particle maintained its spherical configuration all through the process, the temperature of the particle was calculated from the following expression:

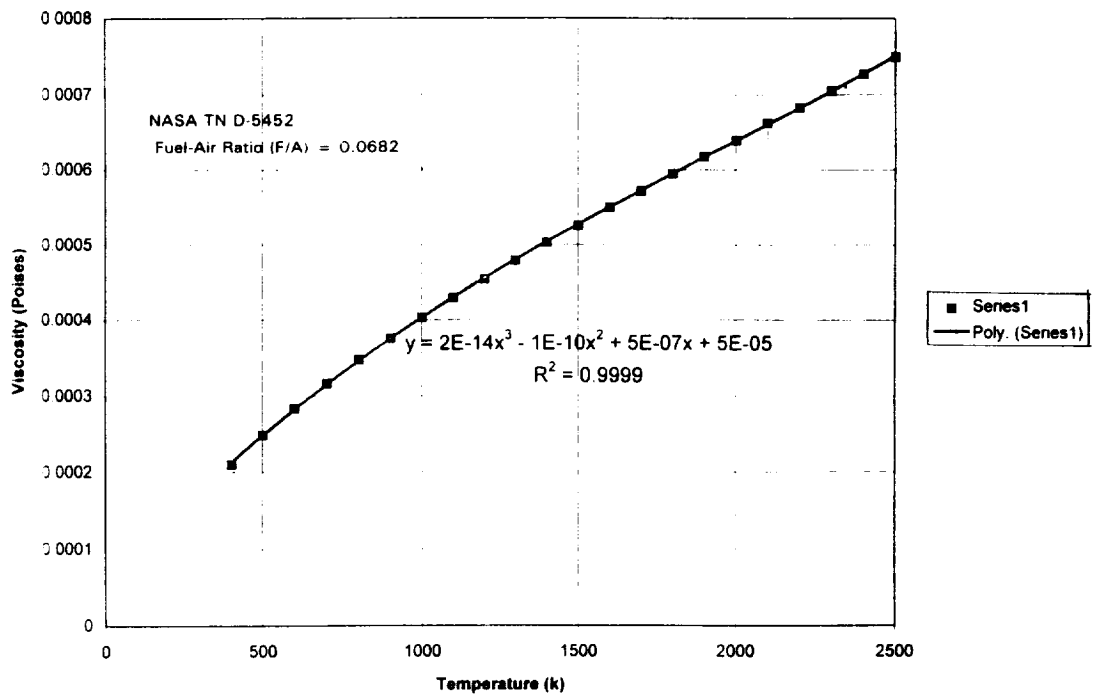


Fig. (5) Viscosity vs Temperature For Combustion Gases of ASTM-A-1 Burned in Air at 3 Atmospheres

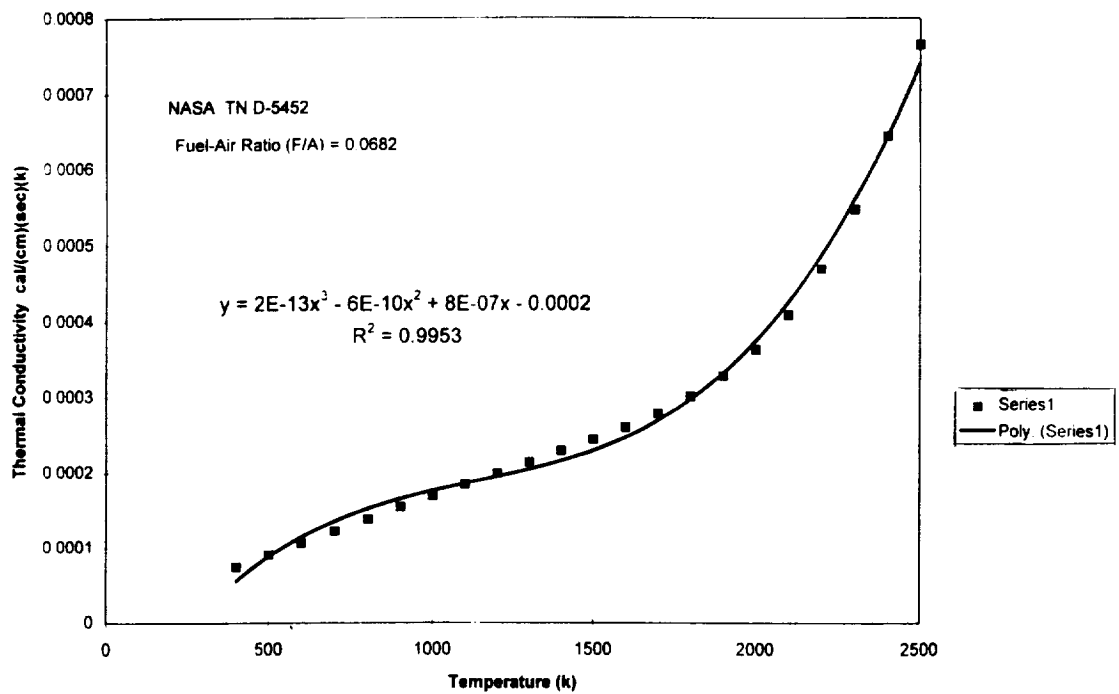


Fig.(6) Thermal Conductivity vs Temperature For Combustion Gases of ASTM-A-1 Burned in Air at 3 Atmospheres

$$T_p = \frac{\Delta t h T_g + \frac{1}{3} \rho_p R_p c_p T_{p_i}}{\Delta t h + \frac{1}{3} \rho_p R_p c_p}$$

3. RESULTS AND ANALYSIS

The model predictions showed an expected sharp increase in both of the particle velocity and temperature when the powder was initially injected in the barrel, Figures (7A)

and (7B). The particle velocity at the end of the barrel was about half the gas velocity at the end of the barrel.

Meanwhile, the particle temperature closely approached the gas temperature at the same section. This indicates that the heat transfer mechanism between the gas and the particle is more efficient than the momentum transfer mechanism. The model predictions of particle and gas velocities and temperatures in the jet plume Figures (7B) and (8B) showed that the gas maintained its velocity and temperature over the potential core zone, that extends up to X/D approximately equals 8 to 10, due to a very small amount of ambient air entrainment. At the end of this zone, both the gas velocity and temperature experience rapid decrease as they cross below the particle velocity and temperature curves shown in Figures(7B) and (8B). This is attributed to large entrainment of a comparatively much cooler and slower surrounding atmosphere in the mixing turbulent region of the jet generated by the shear

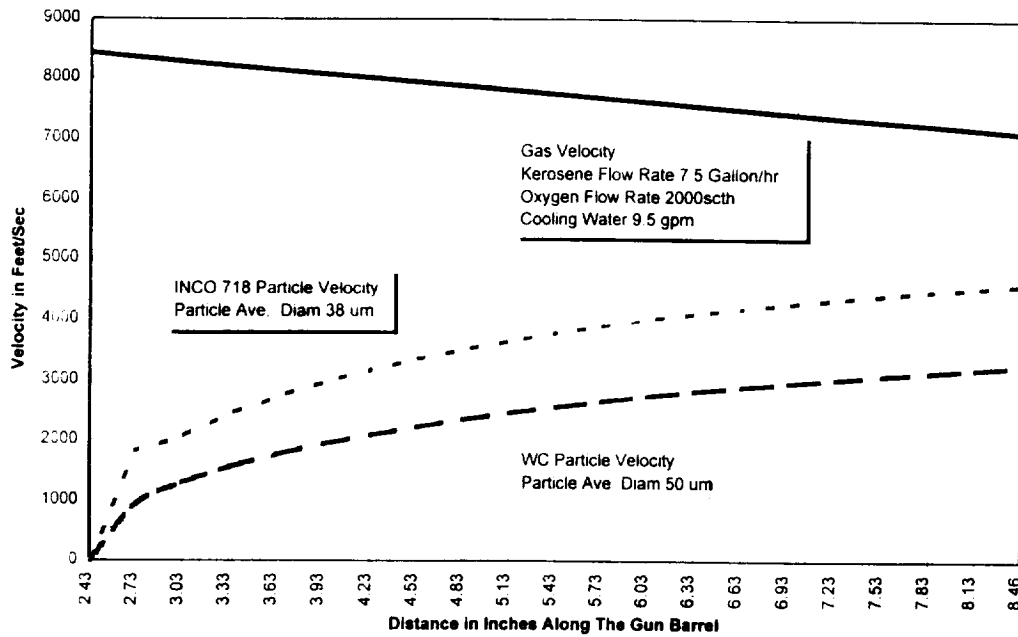


Fig. (7A) Predicted Gas and Particles Velocities Inside The JP-5000 Barrel

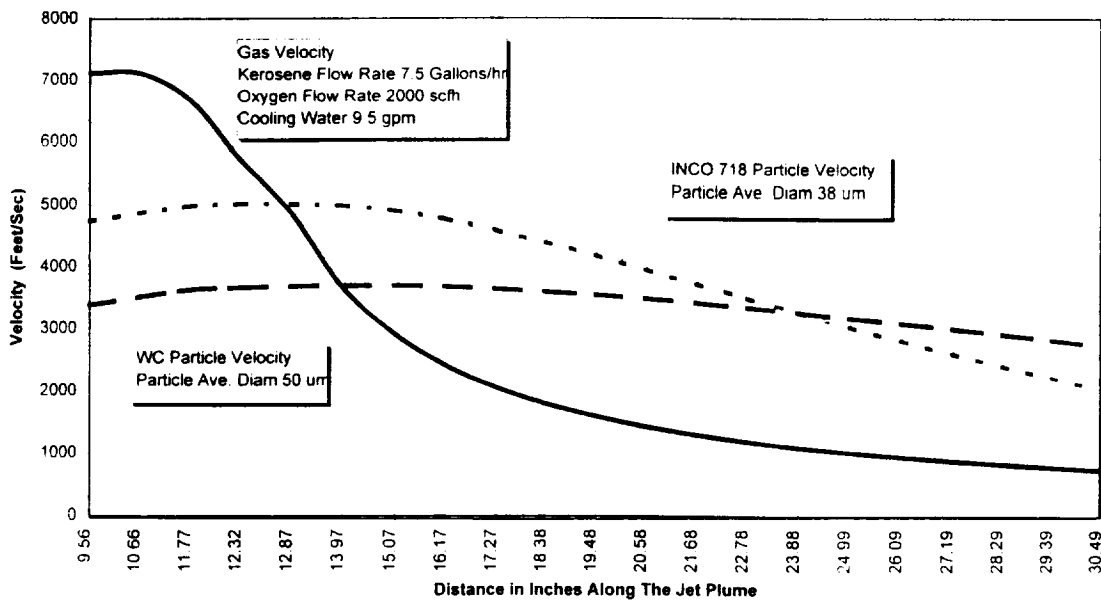


Fig. (7B) Predicted Gas and Particles Velocities In The Free Jet Plume of a HVOF System

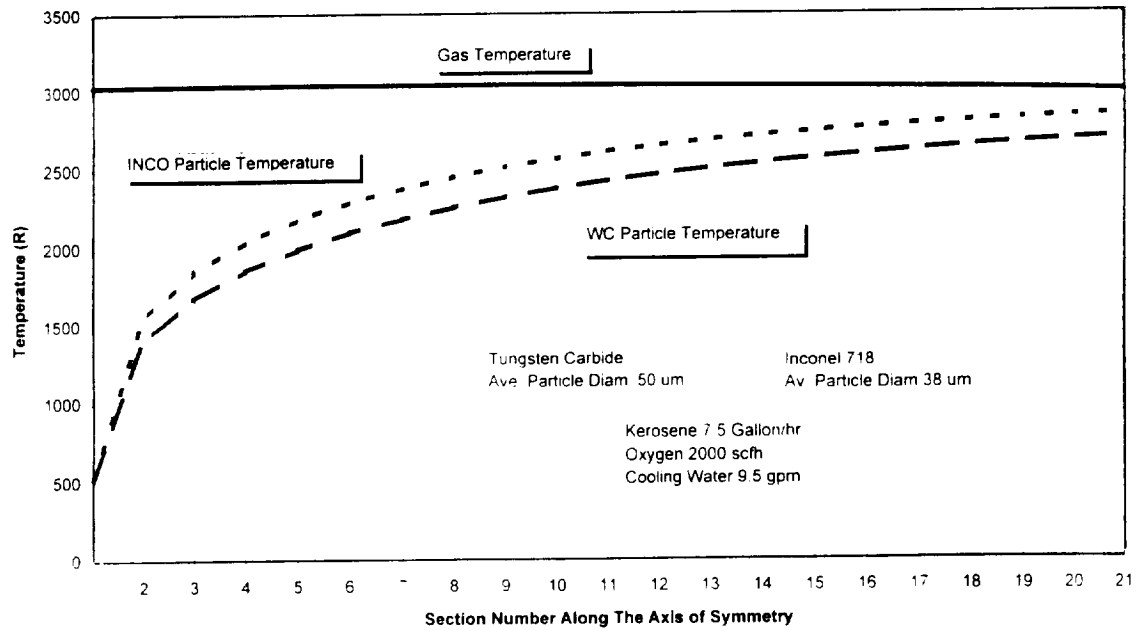


Fig.(8A) Predicted Gas and Powder Temperatures inside The JP-5000 Gun Barrel

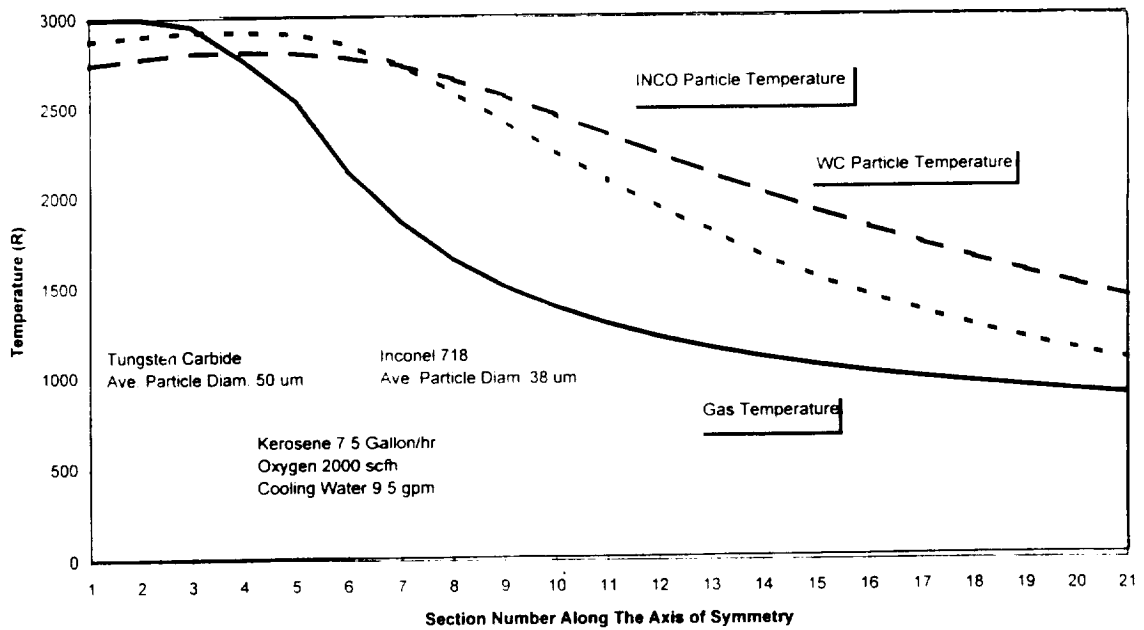


Fig. (8B) Predicted Gas and Powder Temperatures in The Jet Plume

6. RECOMMENDATIONS

- (1) Measurements of velocity and temperature of gas and particle are necessary for the model validation
- (2) The model should be used to perform parametric study and system optimization
- (3) Rectify the singularity problem due to the appearance of the term $(1-M^2)$ in the denominator - Use Taylor series expansion

7. REFERENCES

- [1] R.L.Daniel, H.L. Sanders, M.J. Mendrek, "Replacement of Environmentally Hazardous Corrosion Protection Paints on the Space Shuttle Main Engine Using Wire Arc Sprayed Aluminum", Proceedings of the 7th National Thermal Spray Conference 20-24 June 1994, Boston, Massachusetts.
- [2] P.Siitonen, T.Konos, P.Kettunen, "Corrosion Properties of Stainless Steel Coatings Made by Different Methods of Thermal Spraying", Proceedings of the 7th National Thermal Spray Conference 20-24 June 1994, Boston, Massachusetts.
- [3] R.Shah, K-C.Wang, K.Parthasaathi, J.Jo, E.Onesto, "Towards Manufacturing High-Quality Thermal Spray Coatings", Proceedings of the 7th National Thermal Spray Conference 20-24 June 1994, Boston, Massachusetts.
- [4] O.Knotek, E.Lugscheider, P.Jokiel, U.Schnaut, A.Wiemers, "Chromium Coatings by HVOF Thermal Spraying: Simulation and Practical Results, Proceedings of the 7th National Thermal Spray Conference 20-24 June 1994, Boston, Massachusetts.
- [5] W.D.Swank, J.R.Fincke, D.C.Haggard, G.Irons, R.Bullock, "HVOF Particle Flow Field Characteristics", Proceedings of the 7th National Thermal Spray Conference 20-24 June 1994, Boston, Massachusetts.
- [6] C.M.Hackett, G.S.Settles, "Turbulent Mixing of the HVOF Thermal Spray and Coating Oxidation", Proceedings of the 7th National Thermal Spray Conference 20-24 June 1994, Boston, Massachusetts.
- [7] H.Tawfik, F.Zimmerman, "Quality Optimization of Thermally Sprayed Coatings Produced by HVOF Systems Using Mathematical Modeling", 1994 NASA/ASEE Summer Faculty Fellowship Program, NASA Marshall Space Flight Center, AL.
- [8] J.C.Lau, P.J.Morris, "Measurements in subsonic and supersonic free jets using a laser velocimeter", J. Fluid Mech, (1979), vol. 93, part 1, pp.1-27

- [9] N.T.Lagen, J.M.Seiner,"Evaluation of Water Cooled Supersonic Temperature and Pressure Probes For Application to 2000°F Flows", NASA Technical Memorandum 102612.
- [10] L.Y.Jiang, J.P.Sislian, "LDV Measurements of Mean Velocity Components and Turbulence Intensities in Supersonic High-Temperature Exhaust Plumes", AIAA-93-3067.
- [11] W.L.Oberkampf, M.Talpallikar,"Analysis of a High Velocity Oxygen-Fuel (HVOF) Thermal Spray Torch-Part 1: Numerical Formulation", Proceedings of the 7th National Thermal Spray Conference 20-24 June 1994, Boston, Massachusetts.
- [12] M.L.Thorpe, and H.J.Richter,"A Pragmatic Analysis and Comparison of HVOF Processes", Journal of Thermal Spray Technology, Volume (12) June 1992-161.

